

Effect of *In Situ* Polymerization Conditions of Methyl Methacrylate on the Structural and Morphological Properties of Poly(methyl methacrylate)/Poly(acrylonitrile-*g*-(ethylene-*co*-propylene-*co*-diene)-*g*-styrene) PMMA/AES Blends

Fabiana Pires de Carvalho, Maria do Carmo Gonçalves, Maria Isabel Felisberti

Chemistry Institute, University of Campinas (UNICAMP)13083-970 Campinas, SP, Brazil

Received 23 May 2011; accepted 18 July 2011

DOI 10.1002/app.35337

Published online 3 November 2011 in Wiley Online Library (wileyonlinelibrary.com).

ABSTRACT: In this study, the structural and morphological properties of poly(methyl methacrylate)/poly(acrylonitrile-*g*-(ethylene-*co*-propylene-*co*-diene)-*g*-styrene) (PMMA-AES) blends were investigated with emphasis on the influence of the *in situ* polymerization conditions of methyl methacrylate. PMMA-AES blends were obtained by *in situ* polymerization, varying the solvent (chloroform or toluene) and polymerization conditions: method A—no stirring and air atmosphere; method B—stirring and N₂ atmosphere. The blends were characterized by infrared spectroscopy (FTIR), transmission electron microscopy (TEM), and dynamic mechanical analysis (DMA). The results showed that the PMMA-AES blends are immiscible and present complex morphologies. This morphology shows an elastomeric dispersed phase in a glassy matrix, with inclusion of the matrix in the elastomer domains, suggesting *core shell* or *salami* morphology. The occlusion of the glassy phase within the elastomeric

domains can be due to the formation of graft copolymer and/or phase inversion during polymerization. However, this morphology is affected by the polymerization conditions (stirring and air or N₂ atmosphere) and by the solvent used. The selective extraction of the blends' components and infrared spectroscopy showed that crosslinking and/or grafting reactions occur on the elastomer chains during MMA polymerization. The glass transition of the elastomer phase is influenced by morphology, crosslinking, and grafting degree and, therefore, T_g depends on the polymerization conditions. On the other hand, the behavior of T_g of the glassy phase with blend composition suggests miscibility or partial miscibility for the SAN phase of AES and PMMA. © 2011 Wiley Periodicals, Inc. *J Appl Polym Sci* 124: 2846–2856, 2012

Key words: poly(methyl methacrylate); AES; *in situ* polymerization

INTRODUCTION

Mixing two or more polymers together is an easy way to achieve desired properties without the need to synthesize specialized polymer systems. The design, selection, and performance of polymer blends crucially depend on the ability to predict and to control the phase behavior and the morphology of the blends. Most research on polymer blends has focused on materials prepared by conventional mixing of component polymers; the *in situ* polymerization of polymer blends has occasionally been explored, although one of the most important commercial blends, high impact polystyrene (HIPS), is usually

obtained by using similar procedures.¹ Polymer blends prepared through *in situ* polymerization may possess morphologies that result from reaction-induced phase separation and from a complex combination of the products of crosslinking and grafting reactions, and thus provide the final products with different and, in many cases, superior properties in comparison to materials prepared by other ways. The development of complex morphologies in these blends during the polymerization has been observed to significantly improve final properties such as impact strength.² Another factor influenced by *in situ* polymerization is stereochemistry. In an earlier article, Carvalho et al.³ reported the radical polymerization of the poly(methyl methacrylate), PMMA, in the presence of poly(acrylonitrile-*g*-(ethylene-*co*-propylene-*co*-diene)-*g*-styrene) (AES), resulting in PMMA with increasing amounts of triad syndiotactic as the AES content in the reaction medium increased.

The most commercially significant example of *in situ* polymerization blends is found in the toughening of a brittle polymer by rubber modification.

Correspondence to: M. I. Felisberti (misabel@iqm.unicamp.br).

Contract grant sponsor: FAPESP; contract grant numbers: Proc. 04/13723-1, 2010/02098-0.

HIPS is known as a typical rubber-toughened polymeric material basically prepared by free radical polymerization of styrene in the presence of dissolved polybutadiene (PB). However, many details of its complex physical chemistry properties are still unknown. An indication of the complexity of this system is that so far, no mathematical model of the process has been developed that is capable of predicting the evolution of the particle morphology.⁴

The structural and morphological characteristics of the blend obtained by *in situ* polymerization depends on several variables such as the type and amount of rubber and initiator, polymerization temperature, stirring rate, grafting efficiency, molar mass, concentration of chain transfer, and interfacial surface. The effects of the stirring rate, the temperature, the initiator characteristics, the concentration of chain transfer agent, and the modifier concentrations on the final properties of HIPS have been investigated.⁴⁻⁷ Soto et al.⁴ observed that the rubber particle diameters in HIPS can be made smaller by increasing either the stirring rate or the grafting efficiency. Besides, previous studies have revealed that the size of the rubber particles increases with increasing rubber content, initiator concentration, and chain transfer agent concentration.^{5,6} With relation to the initiator, Soto et al.⁴ observed that peroxide radicals are more efficient for inducing graft copolymerization than azo radicals.

In the standard HIPS process, the generation of graft copolymer during the polymerization is vital because of its effect on morphology and mechanical properties. By accumulating at the interfaces the graft copolymer reduces the interfacial tension, promotes phase inversion, and controls particle size.⁴ The rubber phase in HIPS contains unreacted PB, graft copolymer, and possibly crosslinked PB.⁸

Another blends obtained by *in situ* polymerization have been studied such as PMMA and poly(ethylene-*co*-vinyl acetate) (EVA),⁹ poly(styrene) (PS) and AES,¹⁰ PS and poly(styrene-*b*-butadiene-*b*-styrene) (SBS),⁷ PMMA and poly(styrene-*co*-acrylonitrile) (SAN),¹¹ and PS and poly(ethylene-*co*-propylene-*co*-diene) (EPDM).^{12,13} Cheng and Chen⁹ investigated the influence of the initiator on the morphology of PMMA/EVA blends and observed that the formed graft copolymer results in finely dispersed EVA particles in the PMMA matrix. In general, the mechanical properties of *in situ* polymerized blends are better than the properties of the corresponding blends prepared by melt mixing. This is due to formation of copolymers at the interface, to crosslinking and to the particular morphology of *in situ* polymerized blends.

Poly(acrylonitrile-*co*-butadiene-*co*-styrene) (ABS), HIPS, and poly(methyl methacrylate-*co*-butadiene-*co*-styrene) copolymer (MBS) are efficient impact resist-

ance modifiers, however they present low thermal resistance and low weatherability due to the high level of unsaturation of the rubber phase.^{14,15} This limitation can be overcome by using saturated elastomers like EPDM and AES instead of PB. *In situ* polymerized blends of PS and AES are more thermo and photochemically stable than HIPS, for instance.¹⁶ AES is a very attractive impact resistance modifier for thermoplastics due to comparable impact strength and better environmental and thermal resistance than ABS.^{14,15} AES is a very complex thermoplastic elastomer constituted by free EPDM, free SAN, and a graft copolymer of SAN on EPDM chains.¹⁴

Because of its composition and properties AES is seen as a good and promising candidate for modifying and improving the mechanical properties of PMMA, mainly because the interactions between PMMA and the SAN phase of AES could play an important role in the compatibilization of PMMA-AES blends. This hypothesis is based on the fact that PMMA-SAN blends exhibit a miscibility window. This miscibility window is very well established in the literature and it depends on the molar mass of the polymers, on the temperature, and on the acrylonitrile content in the SAN.¹⁷⁻¹⁹

In this work, PMMA-AES blends were prepared by *in situ* polymerization of methyl methacrylate monomer in the presence of AES to investigate the effect of polymerization conditions on structural and morphological properties. This way, the blends were prepared varying of the solvent type under air or an inert atmosphere. In radical polymerization, the presence of oxygen can affect the reaction kinetics producing species such as polymeric peroxide, for example. This kind of reaction competes with the usual propagation reactions resulting in an inhibition of polymerization.²⁰

EXPERIMENTAL

Materials

Chemtura Corp. supplied AES (Royaltuf® 372P20). AES is a complex mixture of SAN, EPDM, and grafted copolymer EPDM-*g*-SAN. AES contains 13 wt % free EPDM, 22 wt % free SAN, and approximately 65 wt % EPDM-*g*-SAN. SAN presents 27 wt % acrylonitrile content. The global composition of AES is 50 wt % SAN and 50 wt % EPDM. The EPDM of AES contains 68.9 wt % ethylene, 26.5 wt % propylene, and 4.6 wt % 2-ethylidene-5-norbornene (ENB) as diene.²¹ The molar mass (\overline{M}_n) and polydispersity of AES are 448 kg mol⁻¹ and 6, respectively.

Methyl methacrylate monomer (Proquigel Química S/A) was submitted to extraction of

TABLE I
PMMA-AES Blends Prepared in this Work

Solvent	Name	Method	EPDM in the blend (wt %) ^a
Chloroform	6.9EPDM-C-A	A	6.9
	7.9EPDM-C-A	A	7.9
	6.5EPDM-C-B	B	6.5
	9.3EPDM-C-B	B	9.3
Toluene	6.9EPDM-T-A	A	6.9
	11.8EPDM-T-A	A	9.3
	6.5EPDM-T-B	B	6.5
	11.1EPDM-T-B	B	11.1

^a EPDM content in blends calculated from elemental analysis.

polymerization inhibitors with a 5% NaOH solution. After this, the organic layer was washed with distilled water. Then MMA monomer was dried using Na₂SO₄ and distilled at 25°C under vacuum. Methyl methacrylate monomer was stored at -15°C.

In situ polymerization of PMMA-AES blends

The blends were prepared by two different processes, called method A and method B.

Method A: AES was dissolved in chloroform or toluene (1 : 6 w/v) under stirring for 1 h at room temperature. Then methyl methacrylate monomer was added and the mixture was stirred for 48 h before initiating polymerization. Benzoyl peroxide (0.1 wt %) was added to the viscous and homogeneous solution and the polymerization was carried out at 60°C for 192 h.

Method B: AES was dissolved in chloroform or toluene (1 : 6 w/v) under stirring for 1 h at room temperature. Then methyl methacrylate monomer was added and the mixture was stirred for 24 h before polymerization. Benzoyl peroxide (0.1 wt %) was added to the viscous and homogeneous solution and the polymerization was carried out at 60°C under stirring under flowing nitrogen for 8 h. After this time, the stirring was stopped and the reaction mixture was kept under a nitrogen flow until the end of polymerization (around 12 h).

PMMA homopolymer was also prepared by methods A and B. Each polymerization reaction produced cylindrical blocks of 11.0 cm height and 9 cm diameter (approximately 550 g of material). Methyl methacrylate monomer and chloroform or toluene residues were extracted at 120°C in a vacuum oven for 48 h. The yield of the polymerization of methyl methacrylate monomer was around 95% for all composition.

The compositions and the nomenclature used for the PMMA-AES blends are given in Table I. The nomenclature used to describe the blends is based on the EPDM content in the blends and on the polymerization conditions. For example, the blend containing 6.9 wt % of EPDM, polymerized by method

A using toluene (T) as solvent is named 6.9EPDM-T-A, while the blend with similar composition polymerized in CHCl₃ (C) and by method B is called 6.9EPDM-C-B. The AES content in the blends was calculated from the nitrogen percentage determined by elemental analysis.

Selective extraction of the blend's components

The components of the PMMA-AES blends were continuously extracted using a Soxhlet apparatus. Firstly, the EPDM phase was extracted with hexane (named Fraction 1), followed by simultaneous extraction of the PMMA, SAN, EPDM-g-SAN with chloroform (named Fraction 2). Each extraction step was performed for 72 h. The residue of the extraction was named Insoluble Fraction. This procedure was performed in duplicate.

Gel permeation chromatography

The average molar mass (\overline{M}_w), number average molar mass (\overline{M}_n) and polydispersity ($\overline{M}_w/\overline{M}_n$) of Fraction 2 of the PMMA-AES blends were measured by gel permeation chromatography (GPC) in a Waters 510 Gel Permeation Chromatograph with a Waters 410 Differential Refractometer Detector. Separation was performed on polystyrene-divinylbenzene Tosoh-Haas columns with 10 µm particles. High performance liquid chromatography grade THF was used as mobile phase at a flow rate of 1 mL min⁻¹. Standard molar mass polystyrene in the molar range between 9100 g mol⁻¹ and 2,890,000 g mol⁻¹ was used for calibration.

Fourier transformed infrared spectroscopy

Films of Fraction 1, Fraction 2, and Insoluble Fraction were compression molded in a Marconi MA 098/A Hydraulic Press at 180°C at 10 ton and they were characterized by infrared spectroscopy.

Attenuated total reflection spectra of the three fractions were collected using an Illuminat IR (Smiths Detection) equipped with a ZnSe internal reflection element (45°). A spectral range of 4000–650 cm⁻¹ was used with 64 scans collected per spectrum and a resolution of 4 cm⁻¹.

The transmission spectrum of the Insoluble Fraction of the blends was collected using a Fourier transformed infrared spectroscopy (FTIR) Bomem MB-Series spectrophotometer using 16 scans, in the spectral range of 4000–400 cm⁻¹ and a resolution of 4 cm⁻¹.

Transmission electron microscopy

The morphology of the blends was examined in a Carl Zeiss CEM 902 transmission electron

microscope (TEM) associated to electron loss spectroscopy, ESI-TEM. The microscope was operated at an acceleration voltage of 80 kV and equipped with a Castaing-Henry energy filter spectrometer within the column. Ultrathin sections, approximately 40 nm thick, were cut in a Leica EM FC6 cryo-ultramicrotome. Phase contrast between the blend components was achieved by exposing the samples to vapors of OsO₄ for a period of 4 h. The images were recorded using a Proscan high-speed slow-scan CCD camera and processed in the iTEM (Universal Imaging Platform) software.

Dynamic mechanical analysis

Blend specimens of 9.0 mm × 6.0 mm × 1.0 mm dimension were cut from the middle of blocks and submitted to sinusoidal deformation at a frequency of 1.0 Hz and amplitude of 0.02% in the temperature range from -100 to 210°C, at a heating rate of 2 °C/min, in a Rheometric Scientific DMTA V Analyzer.

RESULTS AND DISCUSSION

The solubilization of AES in methyl methacrylate is slow probably because of the high molar mass of AES and viscosity of the resulting solution. To guarantee complete solubilization and homogeneity, a common solvent for both components was used. The solvent used in radical polymerization is known to influence not only polymer characteristics such as coil size and mobility but also many system properties such as viscosity.²² Besides, it is established that the rate of propagation step in radical polymerization can show significant variation according to the solvent employed. Many organic solvents act as chain transfer agents in radical polymerization and their reactivity in transfer reactions depends on the nature of the propagating species.²³ Studies about solvent effect on the radical polymerization of styrene and methyl methacrylate show that chloroform presents a higher transfer constant in comparison with toluene and benzene.²³⁻²⁵ The mechanism of chain transfer for chloroform and toluene in radical polymerization of MMA involves hydrogen abstraction.²⁴

Since the polymerization kinetics and the mechanism of radical polymerization is affected by solvents, a significant impact of the solvent on the morphological and structural features of the blends prepared by *in situ* polymerization is also expected. Therefore, the selection of an appropriate solvent plays a very important role in the preparation of *in situ* polymerized blends.

To investigate the influence of the solvent on methyl methacrylate polymerization, besides morphological and dynamic mechanical analysis (DMA),

selective extraction of the blend's components were carried out. The selective extraction of the blends resulted in three fractions: a hexane soluble fraction (Fraction 1); a chloroform soluble fraction (Fraction 2), and an insoluble fraction (Insoluble Fraction). In principle, the EPDM phase should be extracted with hexane, a non-solvent for PMMA and SAN. PMMA and SAN are soluble in the same solvents making this separation by simple extraction impossible. So, both polymers (PMMA and SAN) were extracted with chloroform (Fraction 2).

The three fractions of the blends were analyzed by infrared spectroscopy (Fig. 1). Figures 1(A-C) show attenuated total reflection infrared spectra of Fraction 1 (extracted with hexane and therefore richer in EPDM), Fraction 2 (extracted with chloroform, richer in SAN and PMMA), and insoluble fraction, respectively, while Figure 1(D) shows the transmission infrared spectra of the Insoluble Fraction of PMMA-AES blends.

The infrared spectra for all fractions present similar bands, but the relative intensity of the bands is different for each fraction. The attenuated total reflection spectra of the Fraction 1, Fraction 2, and Insoluble Fraction show an absorption band at 1377 cm⁻¹, assigned to CH₃ symmetric deformation, another intense band at 1464 cm⁻¹, assigned to CH₂ angular deformation and two intense bands at 2860 and 2960 cm⁻¹, assigned to CH₂ and CH₃ symmetric and antisymmetric stretching of EPDM.^{21,26} The C=O stretching of PMMA at 1724 cm⁻¹, O-CH₃ deformation of PMMA at 1390 cm⁻¹, and the symmetric stretching vibration of the C-O-C bond of PMMA at 990 cm⁻¹ are also observed.²⁷ In the attenuated total reflection spectra, the absorption bands of the acrylonitrile group of SAN (2237 cm⁻¹)²⁶ was not observed in any fractions, because of the low SAN content. However, this characteristic absorption band of the acrylonitrile group can be observed in the transmission infrared spectra of all blends [Fig. 2(D)].

To determine a relative composition of the different fractions of the blends, the absorbance ratio of the CH₂ symmetric stretching band of EPDM and C=O stretching band of PMMA was calculated using the height of each band ($I_{\text{CH}_2}/I_{\text{C}=\text{O}}$). The analysis of the spectra in Figure 1 and the data in Table II allow concluding that Fraction 1 is poorer in PMMA, which means that this phase is constituted of EPDM and PMMA-g-EPDM, while Fraction 2 and Insoluble Fraction are richer in PMMA and probably in SAN. Thus, these results suggest that a little fraction of PMMA is grafted onto the soluble EPDM phase (Fraction 1) and a little fraction of EPDM is grafted and/or crosslinked in the Insoluble Fraction. In addition, the composition Fraction 1 as well as Fraction 2 suggests a higher grafting extent in blends

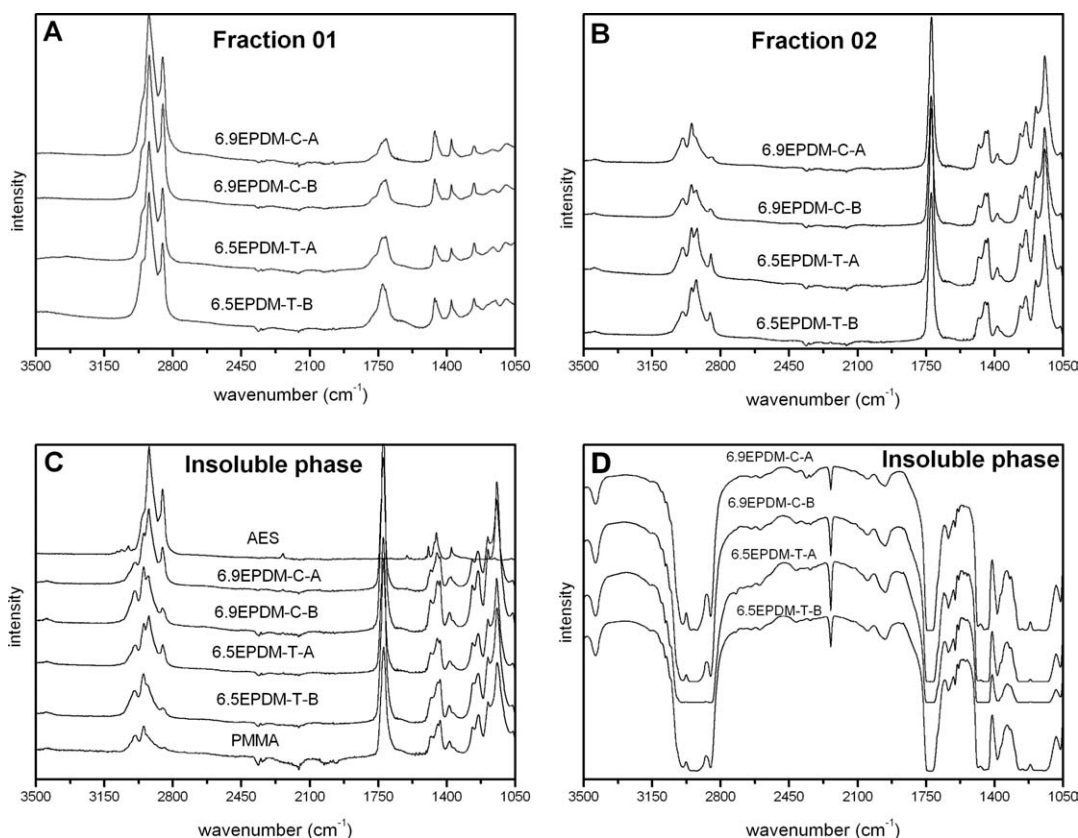


Figure 1 A–C: Attenuated total reflection infrared spectra of extracted PMMA-AES blends of fraction 1, fraction 2 and insoluble phase, respectively. (D) Transmission infrared spectra of extracted PMMA-AES blends of insoluble phase.

prepared in toluene solution. Both, grafting and crosslinking contributed to anchor the elastomer phase to the PMMA matrix. Also, rubber crosslinking is beneficial, since it preserves the particle morphology during material processing.²⁸

As reported by Duin and Dikland,²⁹ crosslinking of EPDM in a radical polymerization medium initiated by peroxide occurs via H-abstraction from the

rubber chains by the radicals formed upon peroxide decomposition, followed by combination or addition of EPDM macroradicals (Fig. 2). Macroradicals on SAN chains can also be formed via H-abstraction from the tertiary carbon of acrylonitrile and styrenic segments³⁰ as shown in Figure 2. All these macroradicals may react with each other as well as with methyl methacrylate and solvent.

All blends prepared by *in situ* polymerization presented an Insoluble Fraction. Table III shows the percentage of Insoluble Fraction, and the average molar mass and polydispersity for the Fraction 2 extracted with chloroform from the PMMA-AES blends. Fraction 2 is a mixture of PMMA and SAN with a small amount of EPDM.

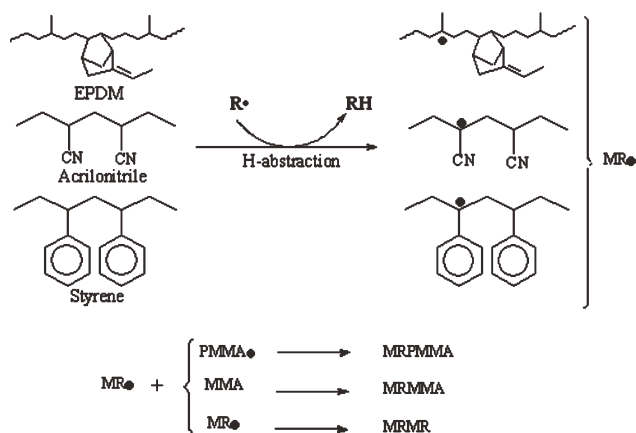


Figure 2 Mechanism of macroradical formation, cross-linking, and grafting reactions of EPDM, SAN, PMMA, and MMA in the presence of peroxide. MR• = macroradical; PMMA• = macroradical of PMMA.

TABLE II
The Absorbance Ratio of CH₂ Symmetric Stretching Band (2860 cm⁻¹) and C=O Stretching Band for Fraction 1, Fraction 2, and Insoluble Fraction

Solvent	Name	$I_{\text{CH}_2}/I_{\text{C=O}}$		
		Fraction 01	Fraction 02	Insoluble Fraction
Chloroform	6.9EPDM-C-A	4.1	0.04	0.3
	6.5EPDM-C-B	3.5	0.08	0.1
Toluene	6.9EPDM-T-A	2.3	0.14	0.2
	6.5EPDM-T-B	1.9	0.16	0.1

TABLE III
Percentage of Insoluble Fraction, Average Molar Mass (\overline{M}_w), and Polydispersity ($\overline{M}_w/\overline{M}_n$) of Fraction 2 of PMMA-AES Blends

Solvent	Name	Insoluble fraction (%)	Fraction 02	
			\overline{M}_w (kg mol ⁻¹)	$\overline{M}_w/\overline{M}_n$
Chloroform	6.9EPDM-C-A	16.1 ± 0.5	172	2.3
	7.9EPDM-C-A	19.2 ± 0.4	204	3.4
	6.5EPDM-C-B	6.3 ± 0.5	302	3.8
	9.3EPDM-C-B	12.6 ± 0.4	283	2.7
Toluene	6.9EPDM-T-A	25.0 ± 0.5	196	3.0
	11.8EPDM-T-A	52.2 ± 0.4	208	3.5
	6.5EPDM-T-B	8.7 ± 0.2	305	3.5
	11.1EPDM-T-B	18.8 ± 0.4	324	1.7

The analysis of the data of Table III allows observing differences in the insoluble Fraction and the molar mass as a function of method and solvent used. The Insoluble Fraction of the blends prepared by method A is higher than the value observed for PMMA-AES blends prepared by method B. During radical polymerization in the presence of oxygen (method A), polymeric peroxides can be formed. These polymeric peroxides can react easily with each other, contributing to the increase of the Insoluble Fraction. In general, independent of the method used, blends prepared in chloroform present higher Fraction 1 than blends prepared in toluene. In relation to molar mass, the results show that Fraction 2 of all blends prepared by method A present lower average molar mass in comparison with Fraction 2 of all blends prepared by method B. The molar mass difference observed for this fraction for each blend should reflect the molar mass difference of the PMMA and also the changes of molar mass of SAN due to grafting of PMMA. Moreover, polymerization in the presence of oxygen (method A), an inhibitor of free radical polymerization,³¹ results in polymers with lower molar mass, as observed. This can be understood based on the fact that the blends prepared in chloroform present lower average molar masses than blends with similar composition prepared in toluene. The MMA + AES + solvent solution is homogeneous, but during MMA polymerization the mixture becomes immiscible. In this complex solution of MMA/PMMA/AES and solvent the solvent acts as a chain transfer agent. The chloroform is a more efficient chain transfer agent than toluene, thus, the expected mass molar should be smaller in chloroform than in toluene for the same degree of conversion of the MMA, what was in fact, observed.

Transmission electron microscopy

Figure 3 shows the TEM micrographs of PMMA-AES blends prepared by method A using chloroform

or toluene as solvent. Since the thin sections were stained with OsO₄ to improve the contrast between the phases, the rubber domains correspond to the dark regions. The micrographs show the morphology of the elastomer phase dispersed in the matrix. Moreover, many occlusions (matrix subinclusion) in the rubber particles can be seen, suggesting a *core-shell* or *salami* morphology. The occlusions are relatively smaller and more elongated in samples polymerized in chloroform by method A, whereas the occlusions are larger and semispherical in samples polymerized in toluene by method A.

The glassy phase occlusions within the elastomeric domains could be originated by the formation of graft copolymer and/or phase inversion during polymerization.^{6,32} Choi et al.³³ studied the effects of the grafting degree on the morphological properties of HIPS obtained by *in situ* polymerization and observed that the presence of grafted chains change the internal structure of rubber particles, i.e., with increasing grafting degree, the observed occlusion in HIPS morphology becomes larger.

As discussed previously, the morphology of *in situ* polymerization blends depends on composition, phase separation extension, crosslinking and grafting degree, among others factors. To understand the complexity of an *in situ* polymerized blend, a description of the entire polymerization process should be explained. Initially, the AES/chloroform/methyl methacrylate solution is homogeneous, but as the concentration and molar mass of PMMA increase, phase separation occurs, leading to a continuous phase of AES/chloroform/methyl methacrylate solution and a dispersed phase which can be a complex mixture of PMMA, SAN, EPDM, solvent, and monomer. After phase inversion, the PMMA-rich phase becomes the continuous phase, whereas the AES-rich phase becomes the dispersed phase. As the grafting process proceeds the more stable are the PMMA droplets before inversion, and hence it is expected that PMMA droplets do not coagulated during phase inversion. This leads to a higher

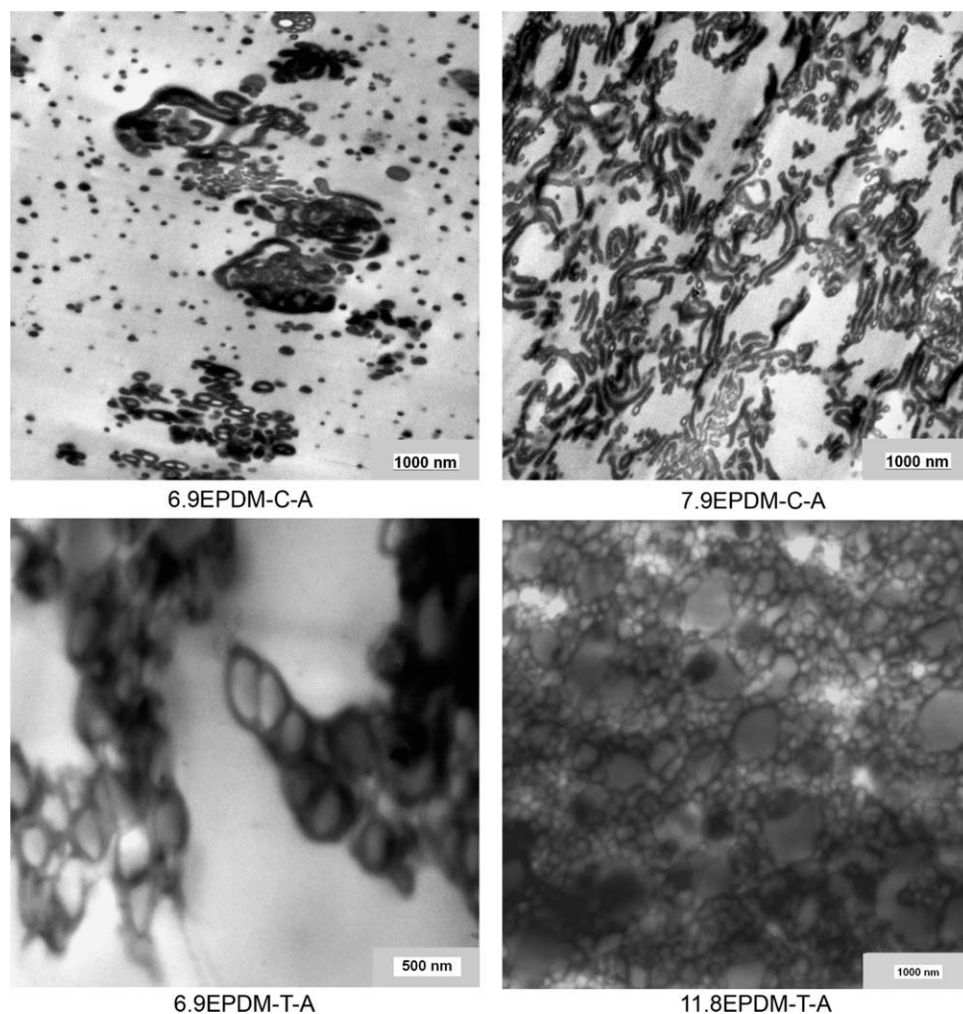


Figure 3 TEM micrographs of PMMA-AES blends prepared by method A using chloroform or toluene as solvent.

fraction of PMMA occlusions in the rubber particles. Thus, the higher occlusion in PMMA-AES blends prepared with toluene is probably due to the presence of a relatively high grafting degree. The graft copolymer reduces the interfacial tension and controls the particle size distribution.²⁸

The blend 7.9EPDM-C-A presents an extraordinary and unique morphology. This kind of morphology is obtained only for blends polymerized *in situ* due to the complexity of the system associated to the evolution of the polymerization process. A very similar morphology was reported by Grego et al. for blends of PA 6.6 and ethylene-propylene rubber.³⁴

Micrographs of the blend 11.8EPDM-T-A, Figure 3, suggest that the elastomer phase is surrounding the glassy polymer phases. This kind of morphology was previously reported in our research group for PS/AES blends also obtained by *in situ* polymerization in the absence of stirring.¹²

Figure 4 shows the TEM micrographs of PMMA-AES blends prepared by method B using chloroform or toluene as solvent. The morphology of the blends

prepared by method B is quite different from the morphology of the blends prepared by method A. The polymerization conditions in Method A and B differ in the atmosphere and stirring, however the influence of stirring on the morphology of the PMMA-AES blends can still be analyzed. As can be seen in Figures 3 and 4 the morphology of the final products prepared under stirring or not is quite different. Recent results of your group showed that the most important factor in determining the morphology of blends of PMMA prepared by *in situ* polymerization is the stirring in comparison with atmosphere.³⁵

In Figure 4 it is possible to observe that blends obtained under stirring present elastomeric particles uniformly distributed in the matrix. As the amount of AES increases, occlusions can also be seen. However, the elastomer is always dispersed phase in the matrix. For these blends, the morphology results not only from phase segregation but also from the mechanism of droplet break up and coalescence, as observed by mechanical dispersion.^{32,30}

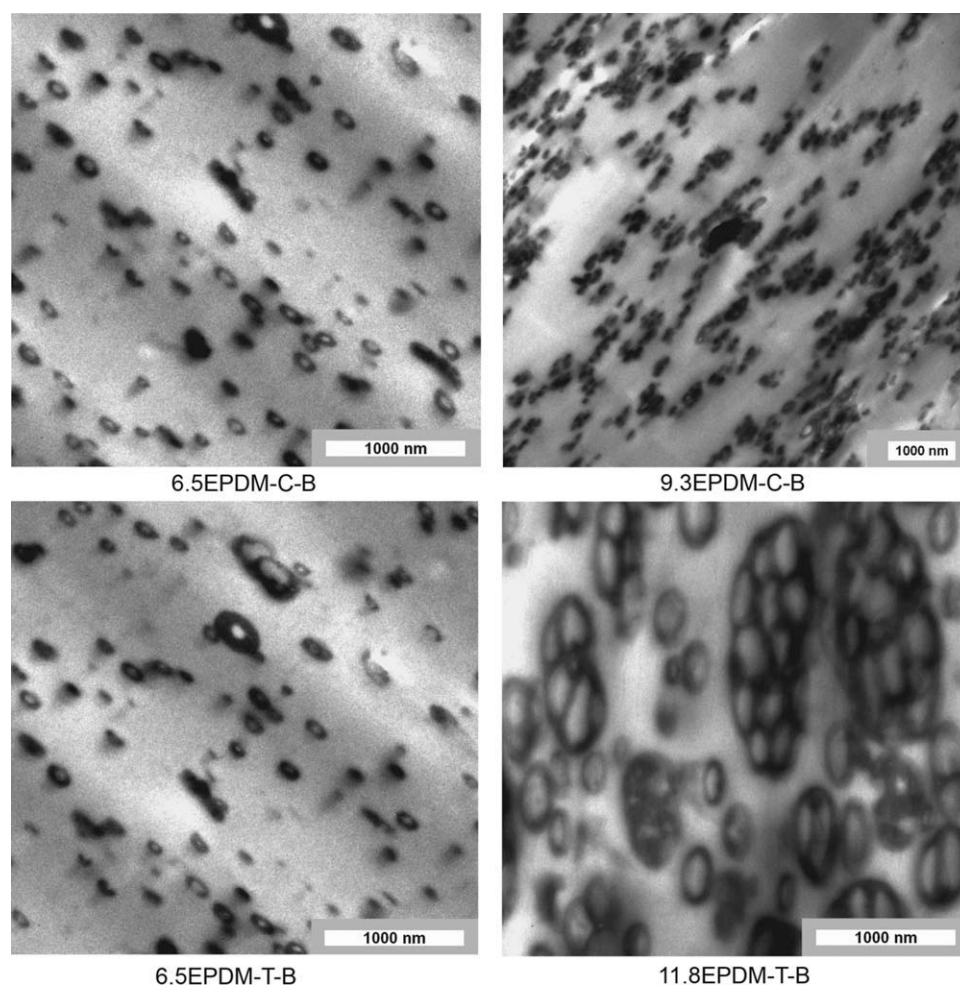


Figure 4 TEM micrographs of PMMA-AES blends prepared by method B using chloroform or toluene as solvent.

Many occlusions can be observed in the 11.1EPDM-T-B blend suggesting *salami* morphology similar to HIPS. Comparing the 6.9EPDM-T-A and 6.5EPDM-T-B blends the following differences can be pointed out: the domain size of the dispersed phase as well as the matrix occlusion fraction in this phase are smaller for the blend prepared under stirring. This can be explained using the mechanism of droplet break up and coalescence that allows the removal of the matrix material from the “elastomer cell.” This effect is more evident comparing the morphologies of the blends 11.8EPDM-T-A (Fig. 3) and 11.1EPDM-T-B (Fig. 4). As discussed previously, these blends do not only differ in morphology, but also in phase composition (Table II) and matrix molar mass (Table III); all these factors influence each other.

Dynamic mechanical analysis

Figure 5 shows the storage modulus (E') as a function of temperature for PMMA, AES, and PMMA-AES blends prepared by method A and method B using chloroform and toluene as solvent.

The E' vs. T curves for PMMA presents a small drop around 0°C corresponding to the β -relaxation of PMMA due to the rotation of the COOCH_3 side chains and another drop above 100°C corresponding to the glass transition.³⁶ For AES, a relaxation can be observed around -40°C associated with the glass transition of the EPDM phase and another relaxation above 110°C attributed to the glass transition of the SAN phase. The storage modulus curves of the PMMA-AES blends show a small drop in the region of the EPDM glass transition and a drop of three decades in the region of the glass transition of the PMMA and SAN phases. The low magnitude of the drop in the storage modulus curves at the glass transition of EPDM phase is in agreement with a morphology of dispersed elastomeric domains (EPDM) in a glassy matrix (PMMA/SAN), as observed by TEM. The loss modulus curves (E'' vs. T , not shown) present peaks at the same temperature range where the storage modulus curves present a drop. The temperatures corresponding to the maximum of these peaks are attributed to the glass transition and shown in Table IV.

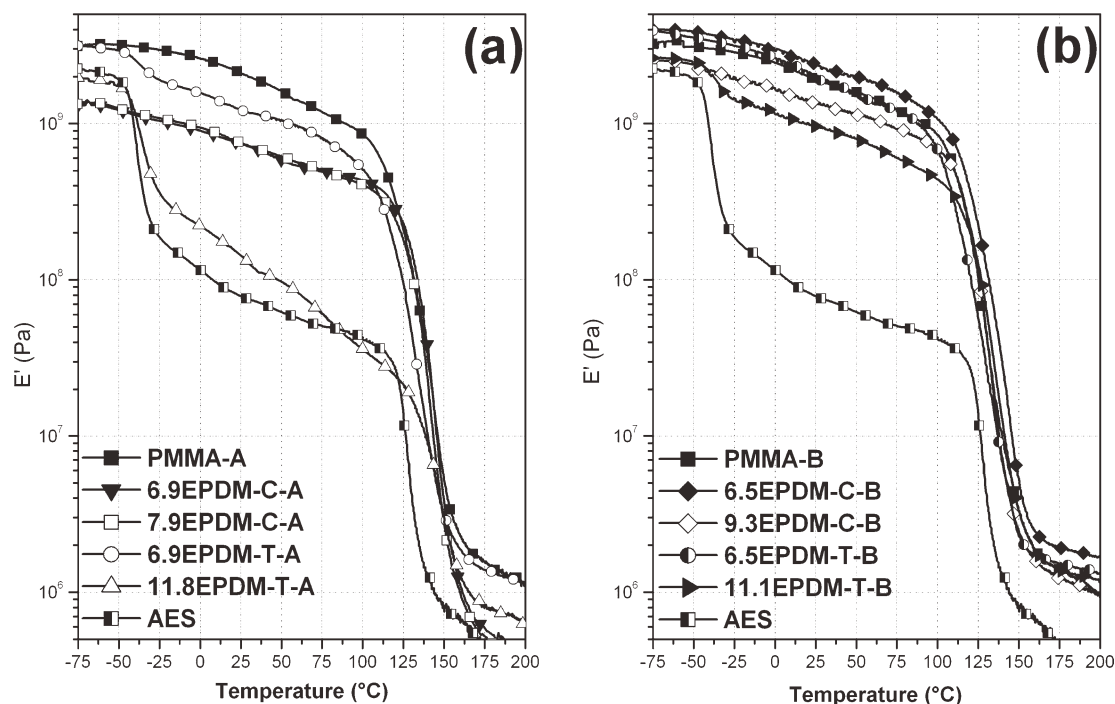


Figure 5 Storage modulus (E') as a function of temperature for PMMA-AES blends prepared by (a) method A, (b) method B.

The EPDM phases of all blends prepared with toluene present a glass transition temperature at higher temperatures than the EPDM phase of AES, while all blends prepared with chloroform present an opposite behavior. This behavior can reflect morphological differences induced by phase separation and also the grafting extent in blends prepared with toluene. Besides as observed by infrared spectroscopy, the selective extraction of Fraction 1 and Fraction 2 shows that these fractions for blends prepared in toluene present different composition in relation to blends prepared in chloroform. This different composition also can explain the higher glass transition temperature observed for blends prepared in toluene.

The shift of the glass transition of the elastomer phase to lower temperatures was also observed in earlier work of our research group for polyhydroxybutyrate/AES blends,³⁷ PMMA/AES blends,³⁸ *in situ* polymerized polystyrene (PS)/AES³⁹ and PS/EPDM.¹² This behavior in blends of a rubbery phase dispersed in glassy material is common and attributed to hydrostatic dilatational thermal stresses generated within the rubber particles because of the differences in the thermal expansion between the rubber and the glass matrix. This dilatational stress promotes an increase in the rubbery phase free volume, which allows reduction of the relaxation time of the rubbery chains and therefore reduces the glass transition temperature of the corresponding phase.^{14,40}

In relation to the glass transition temperature for PMMA/SAN phase for blends with similar compositions the following behavior is observed: blends prepared in chloroform present higher T_g than blends prepared in toluene, independent of the method used. This behavior can be explained due to higher molar mass for blends prepared in chloroform in comparison with blends prepared in toluene and higher grafting degree for blends prepared in toluene.

DMA helps to study polymer/polymer miscibility through analysis of the glass transition of polymers.

TABLE IV
Glass Transition Temperature Obtained from E'' vs. T Curves

Solvent	Materials	Glass transition temperature (°C)	
		PMMA and SAN phases	EPDM phase
Chloroform	PMMA-A	113	–
	PMMA-B	110	–
	AES	122	–41
	6.9EPDM-C-A	129	–43
	7.9EPDM-C-A	123	–51
	6.5EPDM-C-B	114	–42
Toluene	9.3EPDM-C-B	118	–44
	6.9EPDM-T-A	112	–37
	11.8EPDM-T-A	125	–38
	6.5EPDM-T-B	105	–
	11.1EPDM-T-B	120	–36

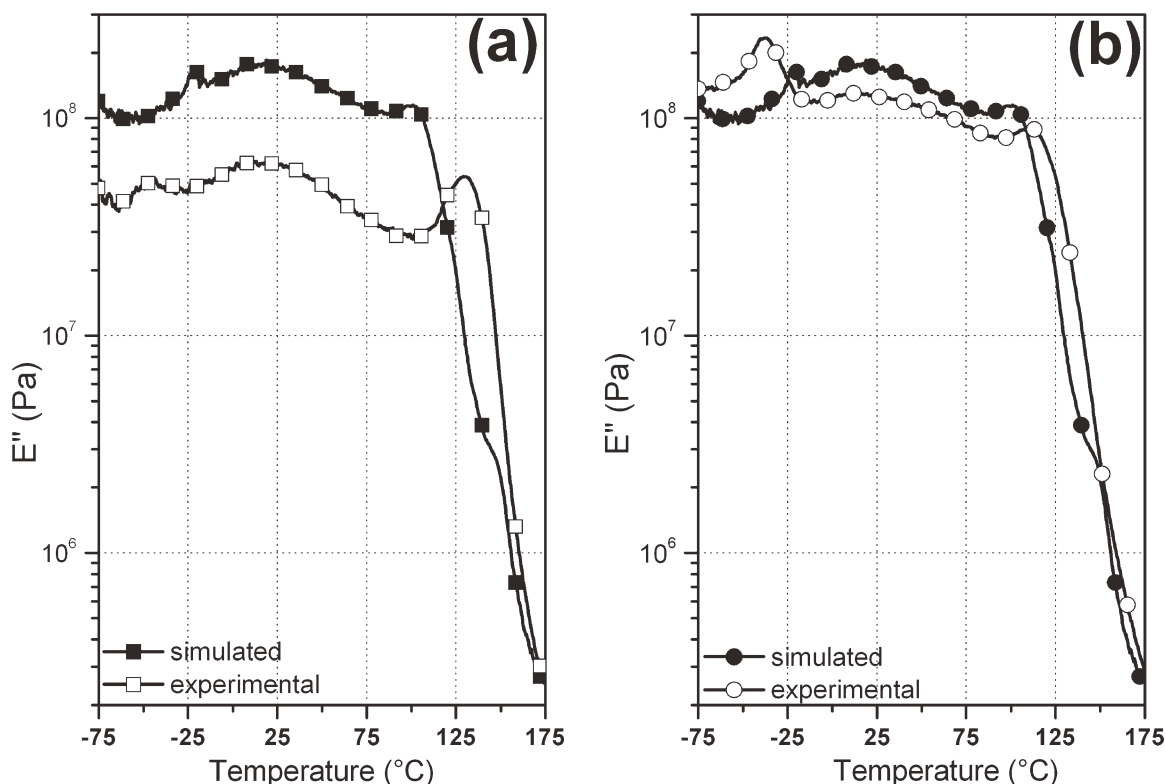


Figure 6 Simulated and experimental E'' vs. T curve and experimental E'' vs. T curve of (a) 6.9EPDM-C-A (b) 6.9EPDM-T-A.

The glass transitions of PMMA and of SAN are close and, because of this the discussion about miscibility can become difficult. One possibility to analyze the miscibility between the PMMA and SAN phases of AES is to simulate the E'' vs. T behavior assuming complete immiscibility of the components of the blends and a morphology of dispersed phase in a matrix. Figure 6 shows the simulated and experimental E'' curves of 6.9EPDM-C-A and 6.9EPDM-T-A. The simulated curve is obtained considering the experimental data for pure components and assuming a morphology of dispersed phase in a matrix.

The simulated E'' curves for 6.9EPDM-C-A and 6.9EPDM-T-A show a peak at 100 $^{\circ}\text{C}$ corresponding to the glass transition of the PMMA phase and a shoulder at higher temperatures corresponding to the SAN phase. However, the experimental E'' curves clearly show a well defined peak with a maximum at intermediate temperature between the maximum of the peak and the shoulder in the simulated E'' curve. This result suggests that there is some degree of miscibility between the PMMA and SAN phases of AES; it may be confined to the interface, resulting in adhesion between the phases. The graft copolymer EPDM-g-SAN should also promote a strong interfacial adhesion between EPDM and the matrix.

The behavior of the glass transition observed for PMMA-AES blends can reflect two possibilities: par-

tial miscibility between PMMA and SAN, since the AN content (27%) of the SAN component used in this work is within the window of miscibility (9.5–33%)^{17,18}; and, less probably overlap of the peaks corresponding to the glass transition of PMMA and SAN phases.

CONCLUSIONS

In situ polymerization is highly multivariate and, for this reason, a large number of reactions must be analyzed to understand the complex interrelationship between preparation conditions such as temperature, type of solvent and initiator used, stirring rate, atmosphere, and structural characteristics, such as conversion, crosslinking degree, grafting efficiency, and morphology. Thus, the choice of preparation conditions is crucial for the properties of the blends.

Chloroform and toluene are known as chain transfer agents for radical polymerization influencing and determining the molecular structure of PMMA, and the grafting and crosslinking degree. These characteristics impact directly on the morphology of the blends. Besides the solvent used, the polymerization conditions (N_2 atmosphere and stirring rate) also influence the morphological properties of the blends. The extent of grafting is the key factor for controlling the whole morphology.

Morphology as well as crosslinking and grafting degree strongly influence the T_g of the EPDM phase of the blends. However, the polymer matrix is probably a miscible or partially miscible blend of SAN and PMMA.

The authors are grateful to Dr. C. H. Collins for manuscript revision.

References

1. Poomalai, P.; Ramaraj, B.; Siddaramaiah. *J Appl Polym Sci* 2007, 104, 3145.
2. Zheng, S.; Guo, Q.; Chan, C. M. *J Polym Sci Part A: Polym Chem* 1999, 37, 2329.
3. Carvalho, F. P.; Gonçalves, M. C.; Felisberti, M. I. *Macromol Symp* 2010, 296, 596.
4. Soto, G.; Nava, E.; Rosas, M.; Fuenmayor, M.; González, I. M.; Meira, G. R.; Oliva, H. M. *J Appl Polym Sci* 2004, 92, 1397.
5. Lee, S. J.; Jeoung, H. G.; Ahn, K. H. *J Appl Polym Sci* 2003, 89, 3672.
6. Estenoz, D. A.; Leal, G. P.; López, Y. R.; Oliva, H. M.; Meira, G. R. *J Appl Polym Sci* 1996, 62, 917.
7. Sardelis, K.; Michels, H. J.; Allen, G. *Polymer* 1987, 28, 244.
8. Casis, N.; Estenoz, D.; Gugliotta, L.; Oliva, H.; Meira, G. *J Appl Polym Sci* 2006, 99, 3023.
9. Cheng, S.-K.; Chen, C.-Y. *J Appl Polym Sci* 2003, 90, 1001.
10. Lourenço, E.; Felisberti, M. I. *J Appl Polym Sci* 2007, 105, 986.
11. Zheng, S.; Li, J.; Guo, Q. *J Mater Sci* 1997, 32, 3463.
12. Lourenço, E.; Gonçalves, M. C.; Felisberti, M. I. *J Appl Polym Sci* 2009, 112, 2280.
13. Lourenço, E.; Felisberti, M. I. *J Appl Polym Sci* 2008, 110, 1804.
14. Larocca, N. M.; Hage, E., Jr.; Pessan, L. A. *Polymer* 2004, 45, 5265.
15. Saron, C.; Felisberti, M. I. *Mater Sci Eng A* 2004, 370, 293.
16. Lourenço, E.; Felisberti, M. I. *Polym Degrad Stab* 2006, 91, 2968.
17. Suess, M.; Kressler, J.; Kammer, H. W. *Polymer* 1987, 28, 957.
18. Kumaraswamy, G. N.; Ranganathaish, C.; Urs, M. V. D.; Ravikumar, H. B. *Eur Polym J* 2006, 42, 2655.
19. Kressler, J.; Higashida, N.; Inoue, T.; Heckmann, W.; Seitz, F. *Macromolecules* 1993, 26, 2090.
20. Bhanu, V. A.; Kishore, K. *J Am Chem Soc* 1991, 91, 99.
21. Turchet, R.; Felisberti, M. I. *Polímeros: Ciência e Tecnologia* 2006, 16, 158.
22. Garcia, M. F.; Martinez, J. J.; Madruga, E. L. *Polymer* 1998, 39, 991.
23. Carraher, C. E., Jr. *Polymer Chemistry*, 6th ed.; Marcel Dekker: New York, 2003.
24. Moad, G.; Solomon, D. H. *The Chemistry of Radical Polymerization*, 2nd ed.; Elsevier Science: San Diego, 2006; Chapter 6.
25. Basu, B. S.; Sen, J. N.; Palit, S. R. *Proc R Soc London A* 1950, 202, 485.
26. Bae, Y. O.; Ha, C. S.; Cho, W. J. *Eur Polym Mater* 1991, 27, 121.
27. Alias, Y.; Ling, I.; Kumutha, K. *Ionics* 2005, 11, 414.
28. Meira, R. G.; Luciani, C. V.; Estenoz, D. A. *Macromol J* 2007, 1, 25.
29. Duin, M. V.; Dikland, H. G. *Rubber Chem Technol* 2003, 76, 132.
30. Grassi, V. G.; Forte, M. M. C.; Pizzol, M. F. D. *Polímeros: Ciência e Tecnologia* 2001, 11, 158.
31. Sideridou, I. D.; Achilias, D. S.; Karava, O. *Macromolecules* 2006, 39, 2072.
32. Leal, G. P.; Asua, J. M. *Polymer* 2009, 50, 68.
33. Choi, J. H.; Ahn, K. H.; Kim, S. Y. *Polymer* 2000, 41, 5229.
34. Grego, R.; Malinconico, M.; Martuscelli, E.; Ragosta, G.; Scarinzi, G. *Polymer* 1987, 28, 1185.
35. Rottela, D. C. Master Dissertation, Institute of Chemistry, University of Campinas, 2011.
36. Xu, F. Y.; Chien, J. C. W. *Macromolecules* 1994, 27, 6589.
37. Carvalho, F. P.; Quental, A. C.; Felisberti, M. I. *J Appl Polym Sci* 2008, 110, 880.
38. Turchet, R.; Felisberti, M. I.; Br, PI. 0305588-4 (2005).
39. Lourenço, E.; Gonçalves, M. C.; Felisberti, M. I. *J Appl Polym Sci* 2009, 113, 2638.
40. Bates, F. B.; Cohen, R. E.; Argon, A. S. *Macromolecules* 1983, 16, 1108.